

# Design, synthesis, and evaluation of 4-(substituted)phenyl-2-thioxo-3,4-dihydro-1*H*-chromino[4,3-*d*]pyrimidin-5-one and 4-(substituted)phenyl-3,4-dihydro-1*H*-chromino[4,3-*d*]pyrimidine-2,5-dione analogs as antitubercular agents

Premlata K. Ambre · Raghuvir R. S. Pissurlenkar ·  
Ravindra D. Wavhale · Mushtaque S. Shaikh · Vijay M. Khedkar ·  
Baojie Wan · Scott G. Franzblau · Evans C. Coutinho

Received: 4 August 2012 / Accepted: 15 October 2013 / Published online: 26 October 2013  
© Springer Science+Business Media New York 2013

**Abstract** This paper focuses on the design and antitubercular activity of molecules which are a hybrid of coumarin and pyrimidine nuclei. A set of 16 compounds, viz. 4-(substituted)phenyl-3,4-dihydro-1*H*-chromino[4,3-*d*]pyrimidine-2,5-diones and 4-(substituted)phenyl-2-thioxo-3,4-dihydro-1*H*-chromino[4,3-*d*]pyrimidin-5-ones have been synthesized using green chemistry principles and evaluated for antitubercular activity by microplate Alamar blue assay (MABA) and luminescence-based low oxygen-recovery assay (LORA) with rifampicin as the standard. The required *Mycobacterium tuberculosis* H37Rv strain for LORA was cultured using a plasmid bearing an *acetamidase* promoter driving a bacterial *luciferase* gene for signal enhancement and were allowed to adapt to low oxygen content in the fermenter. Compounds **5d**, **5e**, and **5g** demonstrated maximum antitubercular activity, with % inhibition values of 58, 55, and 45 based on MABA and 62, 35 and 37 based on the LORA tests at 128  $\mu$ M. To understand the relationship between structure and activity, recursive partitioning (RP) models were developed. Two different RP models were built, one based on the antitubercular activity and the other based on the toxicity of the molecules. The decision tree could identify descriptors that discriminate the active and inactive as well as toxic and less toxic 3,4-annelated coumarin analogs. This RP model will be utilized in further work to design more potent molecules.

**Keywords** 3,4-Annulated coumarins · Antitubercular agents · MABA · LORA · Recursive partitioning (RP)

## Introduction

Tuberculosis (TB) is the world's second leading cause of death as an infectious disease after acquired immune deficiency syndrome (AIDS) (Jindani *et al.*, 1980). The current treatment of TB is an exceedingly lengthy therapy spanning 6–9 months (Jarvis and Lamb, 1998), which makes patient compliance difficult and is a frequent source of drug-resistant strains (Marinis and Legakis, 1985; Cohen and Tartasky, 1997). The need for a lengthy treatment is a consequence of the presence of a population of persistent bacilli that are not effectively eliminated by the current TB drugs (Jarvis and Lamb, 1998; Kawakami *et al.*, 2000). Given the difficulties in successful completion of treatment and the increasing incidences of drug-resistant strains, additional targets for development of new drugs need to be researched (Krajewski *et al.*, 2005). Special efforts are needed to find and develop new leads against the many validated TB targets. New leads with novel modes of action are urgently required to combat the drug-resistant strains of *M. tuberculosis* and stop the emerging TB pandemic (Miyakawa *et al.*, 1996).

Recognizing these needs, we have initiated efforts toward synthesis and screening of diverse heterocyclic entities that have been reported to be active. These are quinolones (Garcia-Garcia *et al.*, 2005), coumarins (McKee *et al.*, 1998; Manvar *et al.*, 2008), imidazopyrans (Stover *et al.*, 2000), phenazines (Barry *et al.*, 1957), substituted triazoles (Shiradkar *et al.*, 2007), phenothiazines (Amaral *et al.*, 2001) pyrimidines, 1,2,3,4-

P. K. Ambre · R. R. S. Pissurlenkar · R. D. Wavhale ·  
M. S. Shaikh · V. M. Khedkar · E. C. Coutinho (✉)  
Department of Pharmaceutical Chemistry, Bombay College of  
Pharmacy, Mumbai 400 098, India  
e-mail: evans@bcplindia.org

B. Wan · S. G. Franzblau  
Tuberculosis Research Centre, University of Illinois, Chicago,  
IL, USA

tetrahydropyrimidines (Desai *et al.*, 2001; Manvar *et al.*, 2010), and pyranocoumarins fused with phenothiazine (Virsdia *et al.*, 2010). Among this heterocyclic group, there are reports of the naturally occurring derivatives of coumarin-like calanolide-A (Spino *et al.*, 1998; Xu *et al.*, 2004) with MIC value of 3.13  $\mu\text{g/ml}$ , and coumarin-4-acetic acid benzylidene hydrazides (Manvar *et al.*, 2008) with  $\text{IC}_{50}$  of 6.25  $\mu\text{g/ml}$  as promising antitubercular agents.

The current work is a continuation of our ongoing search for some new antitubercular agents. Taking into account the fact that coumarins have been reported to possess antitubercular activity and benzopyranopyrimidines are interesting due to their antifungal and antibacterial activities (Kidwai *et al.*, 2006), we hypothesize that their fusion would bring about a synergism in the individual antitubercular activities. Based on the information contained in the steric and electrostatic contours in the CoMFA maps reported in our earlier 3D-QSAR studies on coumarin analogs (Manvar *et al.*, 2008; Virsdia *et al.*, 2010), we have designed, synthesized, and tested 16 molecular variants containing 4-(substituted)phenyl-3,4-dihydro-1*H*-chromino[4,3-*d*]pyrimidine-2,5-diones and 4-(substituted)phenyl-2-thioxo-3,4-dihydro-1*H*-chromino[4,3-*d*]pyrimidin-5-ones and 2-thiopyrimidone nuclei. The compounds have been characterized by IR,  $^1\text{H}$  NMR, and  $^{13}\text{C}$  NMR spectroscopy and evaluated for antitubercular activity based on microplate Alamar blue assay (MABA) and luminescence-based low oxygen-recovery assay (LORA) assays; their cytotoxicity measured *in vitro* on virulent cells. To gain better insight into structure activity relationships, a recursive partitioning (RP) model was developed using physico-chemical, structural, electronic, spatial, thermodynamic, and other descriptors (Blower *et al.*, 2002; Rusinko *et al.*, 2002; Young and Hawkins, 2004; Choi *et al.*, 2006; Strobl *et al.*, 2009).

## Results and discussion

Our earlier 3D-QSAR studies revealed that (Manvar *et al.*, 2008) steric or electronegative substitutions on the coumarin nucleus at the third, fourth, sixth, or seventh positions are favorable for activity, while no modifications are allowed on the lactone ring of the coumarin nucleus. In addition, the same results have also been reported by Virsdia *et al.*, (2010) who showed that bulky substituent at the fourth position of the coumarin increases activity, while Manvar *et al.* (2008, 2010) have reported substituted pyrimidones as potential antitubercular agents. With this knowledge, we have designed a set of 16 compounds with the coumarin ring fused to a thio or oxopyrimidine core viz. 4-(substituted)phenyl-3,4-dihydro-1*H*-chromino[4,3-*d*]pyrimidine-2,5-diones and 4-(substituted)phenyl-2-

thioxo-3,4-dihydro-1*H*-chromino[4,3-*d*]pyrimidin-5-ones as potential antitubercular agents.

## Chemistry

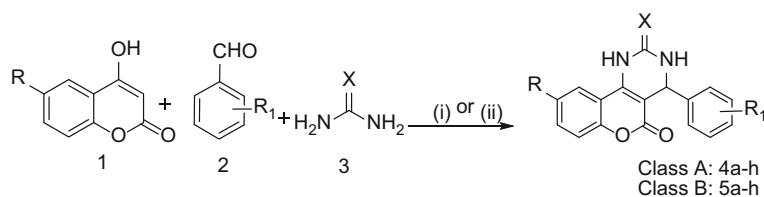
Syntheses of 4-(substituted)phenyl-3,4-dihydro-1*H*-chromino[4,3-*d*]pyrimidine-2,5-diones and 4-(substituted)phenyl-2-thioxo-3,4-dihydro-1*H*-chromino[4,3-*d*]pyrimidin-5-ones were carried out by a three component Biginelli pyrimidone synthesis (Ryabukhin *et al.*, 2011) which involved reaction between a substituted aldehyde, 6-substituted-4-hydroxy coumarin, urea (or thiourea), and an acid catalyst (such as *p*-toluenesulfonic acid) (Scheme 1). The reaction was also successfully worked out using microwave irradiation [discover microwave synthesizer (CEM)] of 850 W microwave power in absence of a solvent for 2.5 min (Scheme 1) in 90 % yields or higher. The structures of the molecules were confirmed by IR,  $^1\text{H}$  NMR, and  $^{13}\text{C}$  NMR spectra; details are given in “Experimental” section. Spectral data (IR,  $^1\text{H}$  NMR, and  $^{13}\text{C}$  NMR) of all the compounds are in full agreement with the proposed structures.

## Biological evaluation

The compounds were screened against *M. tuberculosis* H37Rv strain using the radiometric BECTEC-12B system (Becton Dickinson Diagnostic Instrument System, Sparks, MD, USA) until a growth index (GI) of 800–999 was reached. All compounds were also screened by the MABA (Bartizal *et al.*, 1997) and the LORA (Scott *et al.*, 2007). MABA checks cellular growth and viability of the bacteria while LORA monitors actively replicating as well as non-replicating persistence (NRP) bacteria. Compounds were also checked for cytotoxicity on human virulent cell lines. In both assays, rifampin was the standard drug. The results are summarized in Table 1.

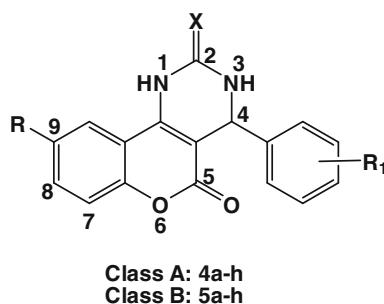
Based on the structures, the molecules are divided into two classes: the phenyl-2-thioxo-3,4-dihydro-1*H*-chromino[4,3-*d*]pyrimidin-5-one (Class A, 4a–h) and the phenyl-3,4-dihydro-1*H*-chromino[4,3-*d*]pyrimidine-2,5-dione (Class B, 5a–h) with eight molecules per class. Majority of Class A molecules are non-cytotoxic based on the human virulent cell lines evaluation with exception of molecules 4g and 4h, although these possess relatively good antitubercular activity against H37Rv cells. The molecules belonging to Class B (5a–h) inhibit growth of *M. tuberculosis* >50 %; however, they have high cytotoxicity profiles.

It is interesting to note that the molecules with the chromino[4,3-*d*]pyrimidine-2,5-dione nucleus (4a and 4e) and molecules 5d, 5e, and 5f have acceptable cytotoxicity and antitubercular activity profiles of which molecule 5d ranks the highest with respect to its activity (MABA 58 %



**Scheme 1** Synthesis of 4-(substituted)phenyl-2-thioxo-3,4-dihydro-1H-chromino[4,3-d]pyrimidin-5-one (**Class A, 4a–h**) and 4-(substituted)phenyl-3,4-dihydro-1H-chromino[4,3-d]pyrimidine-2,5-diones (**Class B, 5a–h**) analogs. (i) Conc. HCl, ethanol, reflux for 12 h; (ii) MW; 850 W, 2.5 min; X = S/O

**Table 1** Structural and experimental information for 4-(substituted)phenyl-2-thioxo-3,4-dihydro-1H-chromino[4,3-d]pyrimidin-2-ones and 4-(substituted)phenyl-3,4-dihydro-1H-chromino[4,3-d]pyrimidine-2,5-diones



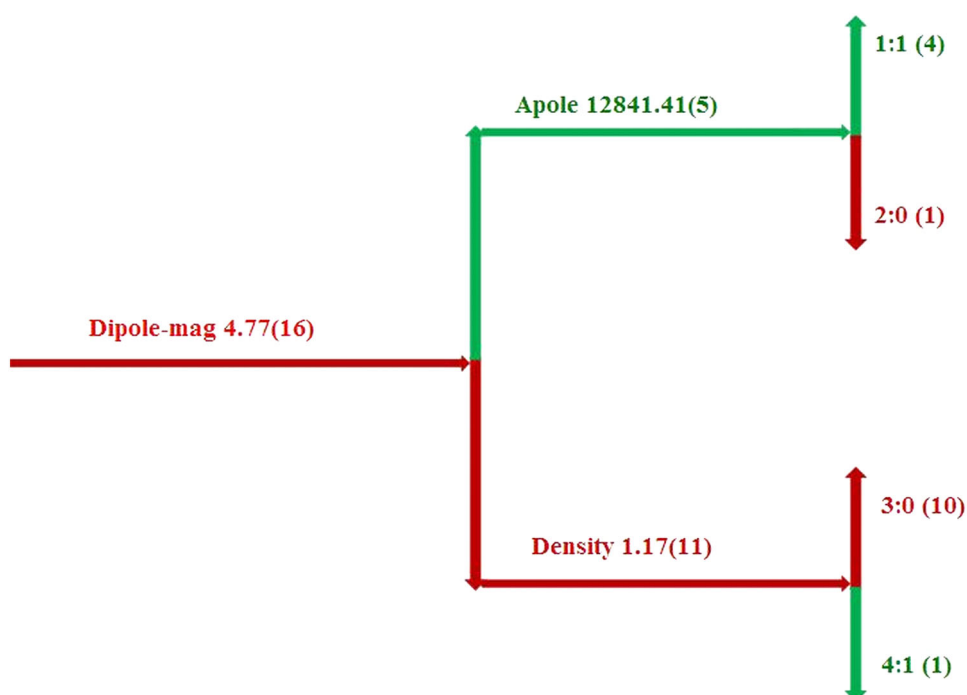
Sl. no.	Class	R	R <sub>1</sub>	X	Percentage yield		Melting point (°C)	MIC (% inhibition @ 128 μM) <sup>a</sup>		IC <sub>50</sub> [μM] vero cell (cytotoxicity)
					Microwave	Conventional		MABA	LORA	
<b>4a</b>	A	H	H	S	92	74	203–205	10	20	>128
<b>4b</b>		H	4-OCH <sub>3</sub>	S	92	76	232–234	0	0	>128
<b>4c</b>		H	3,4-OCH <sub>3</sub>	S	90	73	262–264	0	0	>128
<b>4d</b>		CH <sub>3</sub>	4-OCH <sub>3</sub>	S	90	75	232–234	0	1	>128
<b>4e</b>		CH <sub>3</sub>	3,4-OCH <sub>3</sub>	S	90	75	260–262	9	14	>128
<b>4f</b>		H	3-OCH <sub>3</sub> ; 4-OH	S	92	77	216–218	0	0	>128
<b>4g</b>		H	3-Br	S	94	72	222–224	12	59	47.4
<b>4h</b>		CH <sub>3</sub>	3-Br	S	90	73	232–234	32	61	47.6
<b>5a</b>	B	H	H	O	91	76	210–212	0	17	84.7
<b>5b</b>		H	4-OCH <sub>3</sub>	O	94	72	206–208	8	4	119.2
<b>5c</b>		H	3,4-OCH <sub>3</sub>	O	90	77	262–264	0	0	>128
<b>5d</b>		CH <sub>3</sub>	4-OCH <sub>3</sub>	O	90	79	242–244	58	62	100.7
<b>5e</b>		CH <sub>3</sub>	3,4-OCH <sub>3</sub>	O	94	77	250–252	55	35	>128
<b>5f</b>		H	3-OCH <sub>3</sub> ; 4-OH	O	92	74	208–210	37	1	>128
<b>5g</b>		H	2-OH	O	90	73	242–244	45	37	122.2
<b>5h</b>		H	3-Br	O	90	76	222–224	7	15	106.2

<sup>a</sup> % inhibition recorded at 128 μM concentration for all compounds, MIC of rifampin (standard) used 0.10 and 3.8 μM for MABA and LORA, respectively, against *M. tuberculosis* H37Rv

and LORA 62 %) and cytotoxicity profile (IC<sub>50</sub> = 100.7 μM). The presence of electron donating groups like methyl, methoxy, or hydroxyl on the 4-phenyl ring on the chromino[4,3-d]pyrimidine-2,5-dione nucleus impart greater antitubercular activity while bromine causes

a loss in the activity. A loss in the activity and simultaneously an increased in the cytotoxicity is noted when no substituent is present on the 4-phenyl ring. Molecules that have a methyl substitution at the ninth position of chromino [4,3-d]pyrimidine-2,5-dione nucleus possess greater

**Fig. 1** RP tree generated with moderate pruning: 1:1, 2:0, 3:0, and 4:1, correspond to terminal nodes 1–4 and each terminal node corresponds to the value of 0 (less active) or 1 (active)



antitubercular activity and are devoid of cytotoxicity compared to the unsubstituted analogs.

#### Computational studies

To understand structure–activity relationships, we have built classification models based on the biological activity and cytotoxicity using the technique of RP.

#### RP model for antitubercular activity

RP categorizes the molecules by deriving a binary decision tree in which descriptors are used to split the data set into smaller, homogeneous subsets. A 4-leaf RP decision tree was obtained with 4 terminal and 3 non-terminal nodes for the substituted chrominopyrimidine analogs based on 2D descriptors (vide infra). At each decision point, the tree is split into two branches, higher and lower responses, according to the value of the descriptors. The terminal nodes 1 and 4 contain molecules belonging to Actives class (binary digit 1), while terminal nodes 2 and 3 contain molecules belonging to Inactives class (binary digit 0). The descriptors' dipole moment, radius of gyration, and Apol formed the decision points in the decision tree (Fig. 1). A true response to any given split follows the branch to the downside, while a false response to any given split follow the branch to the upside in a decision tree.

The following 2D descriptors: were calculated using the Cerius2 (Accelrys Inc., USA)—sum of atomic polarizabilities (Apol), dipole moment, radius of gyration, area, molecular weight, molecular volume, density, principal

**Table 2** Descriptors used to develop the RP models

Descriptor	Description
Structural descriptor	The number of H-bond donor and acceptor, number of rotatable bonds, molecular weight
Topological descriptors	Wiener index ( <i>W</i> ), Zagreb index ( <i>Zagreb</i> ), Hosoya index ( <i>Z</i> ), Kier and Hall molecular connectivity index ( $\chi$ )
Spatial descriptors	Radius of gyration, molecular volume, area, density, principal moment of inertia
Electronic descriptors	Charge, Apol, HOMO, LUMO, dipole moment
Thermodynamic descriptors	AlogP98, molecular refractivity

moment of inertia, rotatable bonds, hydrogen bond acceptors, hydrogen bond donors, and AlogP98 (an alternate method for calculating the *o/w* partition coefficient) (Table 2). The dataset was categorized into two sets: the Inactives (0) and the Actives (1). The molecules found to be active by the MABA and LORA assays were classified as actives and rest were classified as inactive. The Inactives set had 11 molecules with <50 % inhibition, while the Actives set had five molecules with >50 % inhibition (the % inhibition being measured at 128  $\mu$ M concentration). The classification model was derived by variation of statistical parameters discussed in the “Materials and methods” section so as to improve the following two aspects.

“Class % Observed Correct”, the so-called intra class prediction providing information on false negatives as well as false positives, depending on the class to be examined;

**Table 3** Statistical results of RP based on antitubercular activity

Class	No. of molecules	% Molecules	Class % observed correct	Overall % predicted correct	Enrichment
1	11	68.75	100	100	1.46
2	5	31.25	100	100	3.20

**Table 4** Antitubercular activity as predicted by the RP model

Sl. no.	Activity	RP-predicted activity	Descriptors		
			Apol	Dipole moment	Density
4a	0	0	13,509.62	3.10	1.20
4b	0	0	14,415.84	4.14	1.20
4c	0	0	15,322.06	2.25	1.20
4d	0	0	14,977.26	4.76	1.18
4e	0	0	15,883.48	2.98	1.18
4f	0	0	14,808.80	4.01	1.22
4g	1	1	13,487.40	8.70	1.41
4h	1	1	14,048.82	10.05	1.38
5a	0	0	12,191.82	3.10	1.18
5b	0	0	13,098.04	4.12	1.18
5c	0	0	14,004.26	2.29	1.18
5d	1	1	13,659.46	4.77	1.16
5e	1	1	14,565.68	2.86	1.16
5f	0	0	13,491.00	4.02	1.20
5g	1	1	12,584.78	5.33	1.21
5h	0	0	12,169.60	8.64	1.40

0 represents inactive while 1 represents active molecule

“Overall % Predicted Correct”, the so-called overall prediction, provides information on the accuracy of the prediction when the whole set is predicted with the model; enrichment factor (ER) for a specific class is the ratio of the “Overall % Predicted Correct” to the original percentage of compounds belonging to that class. The statistical results of the RP model and antitubercular activity predictions from it are summarized in Tables 3 and 4, respectively.

All the 11 molecules of the Inactives set, were correctly classified as *True Negatives*. So also the prediction was 100 % for Actives set, classifying all five molecules as *True Positives*. The ER observed for Actives is 1.46, while that for Inactives is 3.20. The number of true positives among the predictions in each activity set is defined as “Overall % Predicted Correct”. It is noteworthy that for both sets (‘Actives’ and ‘Inactives’), the “Overall % Predicted Correct” was observed to be 100 %. The ER also indicates that the final RP model could be used with confidence for classifying a new library of molecules.

**Table 5** Results of the cross-validation of the RP model for antitubercular activity

Class	Number of compound	%	Class % observed correct	Overall % predicted Correct	Enrichment
1	11	68.75	72.73	88.89	1.29
2	5	31.25	80.00	57.14	1.83

**Table 6** Statistical results of the RP model based on the cytotoxicity data

Class	No. of molecules	% Molecules	Class % observed correct	Overall % predicted correct	Enrichment
1	12	75	100	100	1.33
2	4	25	100	100	4.00

The first primary split occurs on the dipole moment and its value is 4.77. It is an electronic descriptor that indicates the strength and orientation behavior of a molecule in an electrostatic field and has been correlated to long-range ligand–receptor recognition and binding. The dataset is split into two sets with dipole moment above and below 4.77. The classification of the dataset based on dipole moment is shown in Fig. 1.

The next split occurs with the sum of atomic polarizabilities (Apol) and its value is 12,180.71. The terminal node 1 contains four molecules with Apol value >12,180.71 and belong to ‘Actives’, while the remaining 1 molecule has a value below 12,180.71 forming the 2nd terminal node (Fig. 1).

The next split is on density and its value is 1.17. The terminal node 3 contains 10 molecules with density more than 1.17 which is shown as ‘Inactives’ while the remaining 1 molecule with density <1.17 forms the terminal node 4 and is shown in ‘Actives’ (Fig. 1).

In order to avoid over fitting and to improve generalization of the model, internal validation using the technique of tenfold cross-validation which leaves out 10 % of the molecules was carried out. An acceptable classification percentage observed for the sets suggests the stable nature of this model for external testing (Table 5). Considering the size and other limitations in the data set, this prediction rate is acceptable and the key descriptors determined in the trial set are consistent with those observed in the whole set.

#### RP model for cytotoxicity (VCCT)

For building a RP model for cytotoxicity, the set of 16 substituted chrominopyrimidines was categorized into two

**Table 7** The cytotoxicity of the molecules as predicted by the RP model

Sl. no.	VCCT	RP-predicted VCCT	Descriptors		
			Apol	Dipole-mag	Radius of gyration
4a	0	0	13,509.62	3.10	3.73
4b	0	0	14,415.84	4.14	4.12
4c	0	0	15,322.06	2.25	4.35
4d	0	0	14,977.26	4.76	4.36
4e	0	0	15,883.48	2.98	4.55
4f	0	0	14,808.80	4.01	4.23
4g	1	1	13,487.40	8.70	3.76
4h	1	1	14,048.82	10.05	4.04
5a	1	1	12,191.82	3.10	3.72
5b	0	0	13,098.04	4.12	4.11
5c	0	0	14,004.26	2.29	4.35
5d	1	1	13,659.46	4.77	4.35
5e	0	0	14,565.68	2.86	4.55
5f	0	0	13,491.00	4.02	4.23
5g	0	0	12,584.78	5.33	3.75
5h	0	0	12,169.60	8.64	3.75

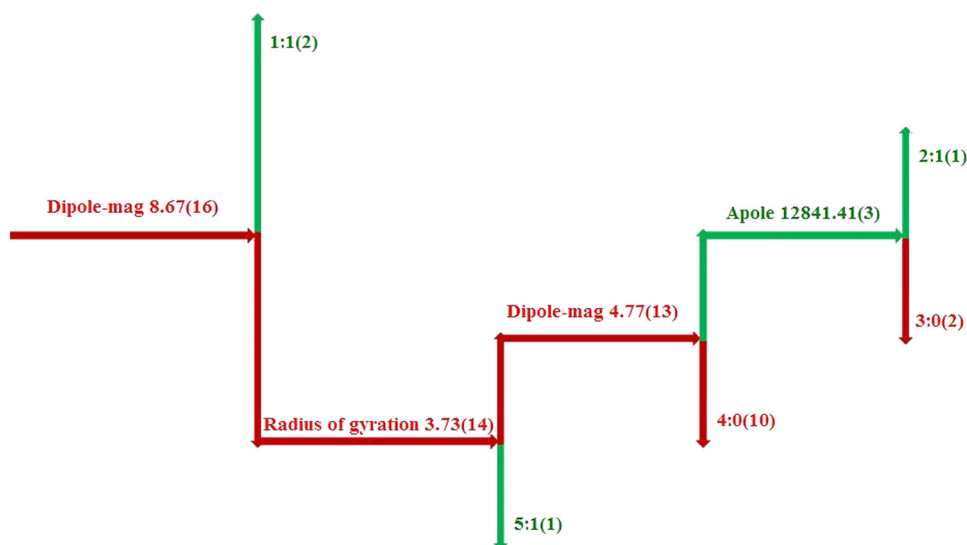
0 represents non-toxic while 1 represents toxic molecule

sets, the ‘Non-toxic’ (binary digit 0) set containing 12 molecules with cytotoxicity  $<100 \mu\text{M}$  ( $\text{IC}_{50}$ ) and the second ‘Toxic’ (binary digit 1) set containing four molecules whose cytotoxicity is  $>100 \mu\text{M}$  ( $\text{IC}_{50}$ ). The molecules have

been evaluated for toxicity on human virulent cell lines. The classification model was derived by variation of parameters discussed in the “Materials and methods” section seeking to improve the following parameters: “Class % Observed Correct”, “Overall % Predicted Correct”, and ER. The statistical outcomes of the RP model and cytotoxicity predictions from it are summarized in Tables 6 and 7, respectively.

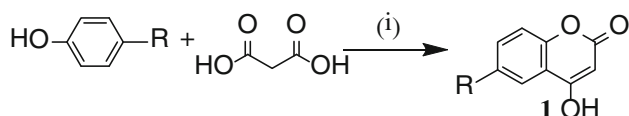
The molecules belonging to the ‘Non-toxic’ and ‘Toxic’ were correctly classified into their corresponding classes of ‘True Positives’ and ‘True Negatives’ with respective ER of 1.33 and 4.00. In a manner similar to the RP model generated for antitubercular activity, a 5-leaf RP decision tree was obtained for the molecules based on the 2D descriptors (Fig. 2). The first primary split based on dipole moment with cutoff 8.67 places 14 molecules as ‘Non-toxic’ and 2 molecules as ‘Toxic’. Further the secondary split based on radius of gyration with cutoff as 3.73, places one molecule as ‘Toxic’ and 13 molecules in ‘Non-toxic’ set. The third split again based on dipole moment at 4.77 places 10 molecules in the ‘Non-toxic’ zone and subsequently the final split based on Apol, with cutoff 12,841.41 places 9 molecules as ‘Non-toxic’. The model was validated to avoid over fitting and to improve generalization of the model. An acceptable classification percentage observed for the classes suggests reasonably good predictability (Table 8). This accuracy in the predictions for the molecules suggests the power of this model for prediction of toxicity of an external set.

**Fig. 2** RP tree generated with moderate pruning: 1:1, 2:1, 3:0, 4:0, and 5:1 correspond to terminal nodes 1–5 and each terminal node corresponds to the value of 0 (less toxic) or 1 (toxic)



**Table 8** Results of the cross-validation of the RP model for cytotoxicity

Class	No. of molecules	% Molecules	Class % observed correct	Overall % predicted correct	Enrichment
1	12	75	75.0	81.8	1.09
2	4	25	50.0	40.0	1.60

**Scheme 2** Synthesis of 6-substituted-4-hydroxycoumarin analogs. Zinc chloride, phosphorus oxychloride, 60–65 °C, 35 h

## Conclusions

A set of 16 molecules belonging to 4-(substituted)phenyl-3,4-dihydro-1*H*-chromino[4,3-*d*]pyrimidine-2,5-diones and 4-(substituted)phenyl-2-thioxo-3,4-dihydro-1*H*-chromino[4,3-*d*]pyrimidin-5-ones were synthesized using microwave irradiation in 90–96 % yield, higher than that obtained by the conventional method (72–79 %). All molecules were assayed against *M. tuberculosis* H37Rv strain using rifampicin as the standard by the MABA and LORA procedures to determine the MIC values. The molecules were also evaluated for cytotoxicity; conducted on human virulent cell lines. Based on results from the MABA and LORA studies, molecules with the phenyl-3,4-dihydro-1*H*-chromino[4,3-*d*]pyrimidine-2,5-dione nucleus are more potent than those with phenyl-2-thioxo-3,4-dihydro-1*H*-chromino[4,3-*d*]pyrimidin-5-one nucleus. The former class is also identified as non-cytotoxic, compared to the latter. Electron donating groups like methyl/methoxy when placed at the ninth position of the 3,4-annelated coumarin nucleus and a 4-methoxy group on the 4-phenyl ring of the chromino core (e.g., **5d**, **5e**, **5g**) improve potency in terms of inhibition of *M. tuberculosis* H37Rv strain and further such derivative are also seen to be non-cytotoxic. A RP model has been developed and is able to accurately classify molecules as active/inactive or toxic/non-toxic.

The molecules were synthesized based on the hypothesis that a fusion of the coumarin and pyrimidin-2,5-dione nuclei both of which cores have been shown to be active against tuberculosis, would give potent antitubercular agents. Indeed the fusion of chromino nucleus with the pyrimidine framework has revealed a novel core and some promising molecules. Molecules **5d**, **5e**, **5g** are worthy of being considered for further development.

## Experimental

An earlier 3D-QSAR study (Manvar *et al.*, 2008) conducted on coumarin-4-acetic acid benzylidene hydrazides and 4-(arylamino)coumarins was the starting point in the design of new and more potent coumarin analogs. Prominent steric contours were observed on the phenyl ring of the benzylidene hydrazide moiety as well as on the 4-(arylamino)coumarin ring which indicated that substituents such as methoxy and bromo would improve the anti-tubercular activity.

The wealth of information in the CoMFA steric and electrostatic contours was used to design some new coumarins analogs by cyclising the coumarin ring at the third and fourth positions with urea and thiourea groups to produce 4-(substituted)phenyl-3,4-dihydro-1*H*-chromino[4,3-*d*]pyrimidine-2,5-diones and 4-(substituted)phenyl-2-thioxo-3,4-dihydro-1*H*-chromino[4,3-*d*]pyrimidine-5-ones.

## Chemistry

All compounds were characterized and their structures confirmed by spectral properties. Solvents and reagents used for synthesis were of laboratory grade. All reactions were monitored by thin layer chromatography using Merck precoated silica plates (GF<sub>254</sub>). Melting points were recorded in open capillaries on an electrically heated ThermoNik melting point apparatus and are uncorrected; boiling points were recorded in a Thiel's tube. IR spectra were recorded (KBr disk method) on a JASCO FT-IR 5300 spectrophotometer. <sup>1</sup>H NMR spectra were recorded on a Bruker AN 300 MHz instrument and <sup>13</sup>C NMR were recorded on a Bruker Advanced II 400 MHz instrument (for compounds **4a–4c**, **4e–4h**, **5a–5c**, **5e**, **5g**, **5h**) and Varian Mercury Plus 400 MHz instrument (for **4d**, **5d**, **5f**). Spectra Chemical shifts are reported in parts per million (ppm) down field from tetramethylsilane (TMS) as the internal standard. The synthetic outline is given in the schemes and detailed procedures are given below.

### General method for synthesis of 6-substituted-4-hydroxycoumarin (Scheme 2)

A mixture of 1.35 g (14.5 mmol) of phenol, 5.95 g (43.7 mmol) of anhydrous ZnCl<sub>2</sub>, 4 ml (0.043 mol) of phosphorus oxychloride, and 1.50 g (0.014 mol) of malonic acid was heated to 60–65 °C. On completion of the reaction (30–35 h), the reaction mixture was cooled and poured on to 50–60 ml cold water and kept aside for 2–3 h till the product precipitated out. The precipitate was filtered and dissolved in saturated solution (~50 ml) of sodium bicarbonate and then acidified with 10 % glacial acetic acid

to pH 2–3 with continuous stirring; the precipitated crude compound (**1**) was crystallized using aq. methanol (yield 60 %).

*General procedure for the synthesis of 4-(substituted)phenyl-3,4-dihydro-1H-chromino[4,3-d]pyrimidine-2,5-dione (4a–h) and 4-(substituted)phenyl-2-thioxo-3,4-dihydro-1H-chromino[4,3-d]pyrimidin-2-one (5a–h) (Table 1; Scheme 1)*

- (i) Conventional approach: A mixture of 600 mg (1.5 mEq) of substituted 4-hydroxycoumarin (**1**), 250 mg (1 mEq) of substituted benzaldehyde (**2**), and 144 mg (1 mEq) of urea or thiourea (**3**) in 20 ml of ethanol containing 4 drops of concentrated hydrochloric acid was heated under reflux for 12 h or until completion of the reaction. The mixture was kept aside for several hours at room temperature and the crude product (**4a–h** or **5a–h**) which precipitated out was filtered, washed with cold methanol (3 × 10 ml) dried and re-crystallized from aqueous methanol.
- (ii) Microwave-assisted approach (Kidwai *et al.*, 2006) (Scheme 1): A mixture of 600 mg (1.5 mEq) of substituted 4-hydroxycoumarin, 250 mg (1 mEq) of substituted benzaldehyde and 144 mg (1 mEq) of urea or thiourea with a catalytic amount of 4-methylbenzenesulfonic acid was placed in a 25-ml round bottom flask and irradiated with microwave at 850 W for 2.5 min [discover microwave synthesizer (CEM)]. After the completion of the reaction, the resulting sticky material was treated with a few drops of methanol 4–5 times and then filtered. The product was then purified by recrystallization from aqueous methanol.

*4-Phenyl-2-thioxo-3,4-dihydro-1H-chromino[4,3-d]pyrimidin-5-one (4a)* IR (KBr,  $\text{cm}^{-1}$ ): 3,402 (N–H), 1,668 (C=O), 1,568 (aromatic C=C bending), 1,278 (C=S).  $^1\text{H}$  NMR ( $\text{CDCl}_3$ ,  $\delta$  ppm): 6.10 (s, 1H, (NH)–C–H), 7.23–7.39 (m, 5H, Ar–H), 7.61 (m, 2H, Ar–H), 8.00 (m, 2H, Ar–H), 11.30 (s, 1H, NH), 11.52 (s, 1H, NH).  $^{13}\text{C}$  NMR ( $\text{CDCl}_3$ ,  $\delta$  ppm): 36.20, 103.92, 105.66, 116.65, 124.40, 124.90, 126.49, 126.89, 128.65, 132.87, 135.22, 152.31, 152.53, 164.59, 165.80, 166.80, 169.30.

*4-Anisyl-2-thioxo-3,4-dihydro-1H-chromino[4,3-d]pyrimidin-5-one (4b)* IR (KBr,  $\text{cm}^{-1}$ ): 3,072 (N–H), 2,837 (aromatic C–H stretch), 1,670 (C=O), 1,510 (aromatic C=C bending), 1,259 (C=S), 1,163 (C–O).  $^1\text{H}$  NMR ( $\text{CDCl}_3$ ,  $\delta$  ppm): 3.80 (s, 3H, (O)–C–H), 6.05 (s, 1H, (NH)–C–H), 6.86–7.26 (m, 4H, Ar–H), 7.63–8.05 (m, 4H, Ar–H), 11.49 (s, 2H, NH).  $^{13}\text{C}$  NMR (DMSO- $d_6$ ,  $\delta$  ppm): 34.95, 54.79,

104.53, 113.49, 115.97, 116.65, 123.72, 123.98, 127.54, 129.28, 132.12, 151.95, 157.59, 163.89, 165.36.

*4-(3,4-Dimethoxy)phenyl-2-thioxo-3,4-dihydro-1H-chromino[4,3-d]pyrimidin-5-one (4c)* IR (KBr,  $\text{cm}^{-1}$ ): 3,439 (N–H), 2,935 (aromatic C–H stretch), 1,664 (C=O), 1,564 (aromatic C=C bending), 1,248 (C=S), 1,140 (C–O).  $^1\text{H}$  NMR ( $\text{CDCl}_3$ ,  $\delta$  ppm): 3.73 (s, 3H, (O)–C–H), 3.87 (s, 3H, (O)–C–H), 6.11 (s, 1H, (NH)–C–H), 6.71–6.81 (m, 3H, Ar–H), 7.64–8.03 (m, 4H, Ar–H), 11.44 (s, 2H, NH).  $^{13}\text{C}$  NMR (DMSO- $d_6$ ,  $\delta$  ppm): 35.36, 55.40, 55.58, 104.47, 111.01, 111.35, 111.95, 116.98, 118.73, 123.73, 123.85, 130.63, 131.97, 147.23, 148.55, 152.02, 164.22, 165.13.

*4-(4-Methoxy)phenyl-9-methyl-2-thioxo-3,4-dihydro-1H-chromino-[4,3-d]pyrimidin-5-one (4d)* IR (KBr,  $\text{cm}^{-1}$ ): 3,210 (N–H), 2,930 (aromatic C–H stretch), 1,672 (C=O), 1,575 (aromatic C=C bending), 1,267 (C=S), 1,109 (C–O).  $^1\text{H}$  NMR (DMSO- $d_6$ ,  $\delta$  ppm): 2.44 (s, 3H, (Ar)–C–H), 3.79 (s, 3H, (O)–C–H), 6.03 (s, 1H, (NH)–C–H), 6.84–7.26 (m, 4H, Ar–H), 7.41–7.83 (m, 3H, Ar–H), 11.33 (s, 1H, NH), 11.55 (s, 1H, NH).  $^{13}\text{C}$  NMR (DMSO- $d_6$ ,  $\delta$  ppm): 20.44, 54.95, 104.44, 113.57, 115.84, 117.00, 123.43, 127.73, 130.70, 132.96, 133.22, 150.23, 157.44, 164.47, 165.07.

*4-(3,4-Dimethoxy)phenyl-9-methyl-2-thioxo-3,4-dihydro-1H-chromino-[4,3-d]pyrimidin-5-one (4e)* IR ((KBr,  $\text{cm}^{-1}$ ): 3,270 (N–H), 2,953 (aromatic C–H stretch), 1,664 (C=O), 1,574 (aromatic C=C bending), 1,267 (C=S), 1,143 (C–O).  $^1\text{H}$  NMR (DMSO- $d_6$ ,  $\delta$  ppm): 2.46 (s, 3H, (Ar)–C–H), 3.73 (s, 3H, (O)–C–H), 3.86 (s, 3H, (O)–C–H), 6.69–6.79 (m, 3H, Ar–H), 6.05 (s, 1H, (NH)–C–H), 7.30–7.41 (m, 2H, Ar–C–H), 7.78–7.84 (m, 2H, Ar–C–H), 11.33 (s, 1H, NH), 11.57 (s, 1H, NH).  $^{13}\text{C}$  NMR (DMSO- $d_6$ ,  $\delta$  ppm): 20.50, 35.35, 55.41, 55.60, 104.46, 110.98, 111.40, 115.78, 116.38, 118.70, 123.33, 130.26, 133.02, 133.34, 147.30, 148.59, 150.15, 163.92, 165.39.

*4-(4-Hydroxy-3-methoxy)phenyl-9-methyl-2-thioxo-3,4-dihydro-1H-chromino-[4,3-d]pyrimidin-5-one (4f)* IR (KBr,  $\text{cm}^{-1}$ ): 3,497 (O–H), 3,070 (N–H), 2,970 (aromatic C–H stretch), 1,666 (C=O), 1,564 (aromatic C=C bending), 1,269 (C=S), 1,128 (C–O).  $^1\text{H}$  NMR ( $\text{CDCl}_3$ ,  $\delta$  ppm): 3.75 (s, 3H, (O)–C–H), 5.61 (s, 1H, (Ar)–O–H), 6.07 (s, 1H, (NH)–C–H), 6.73–6.86 (m, 3H, Ar–C–H), 7.63–8.05 (m, 4H, Ar–C–H), 11.31 (s, 1H, NH), 11.53 (s, 1H, NH).  $^{13}\text{C}$  NMR (DMSO- $d_6$ ,  $\delta$  ppm): 35.21, 55.65, 104.55, 110.62, 115.10, 115.95, 116.26, 118.87, 123.65, 124.09, 127.13, 132.14, 144.97, 147.33, 151.85, 163.79, 165.99.

4-(3-Bromo)phenyl-2-thioxo-3,4-dihydro-1H-chromino[4,3-d]pyrimidin-5-one (**4g**) IR (KBr,  $\text{cm}^{-1}$ ): 3,069 (N–H), 2,719 (aromatic C–H stretch), 1,664 (C=O), 1,564 (aromatic C=C bending), 1,267 (C=S), 763 (C–Br).  $^1\text{H}$  NMR ( $\text{CDCl}_3$ ,  $\delta$  ppm): 6.06 (s, 1H, (NH)–C–H), 7.17–7.34 (m, 4H, Ar–C–H), 7.64–8.05 (m, 4H, Ar–C–H), 11.29–11.57 (s, 2H, NH).  $^{13}\text{C}$  NMR ( $\text{DMSO}-d_6$ ,  $\delta$  ppm): 35.55, 103.84, 116.00, 116.83, 121.83, 123.83, 123.92, 125.63, 128.82, 129.23, 129.95, 132.15, 141.40, 152.06, 164.43, 165.13.

4-(3-Bromo)phenyl-9-methyl-2-thioxo-3,4-dihydro-1H-chromino[4,3-d]pyrimidin-5-one (**4h**) IR (KBr,  $\text{cm}^{-1}$ ): 3,412 (N–H), 2,918 (aromatic C–H stretch), 1,658 (C=O), 1,577 (aromatic C=C bending), 1,269 (C=S), 785 (C–Br).  $^1\text{H}$  NMR ( $\text{DMSO}-d_6$ ,  $\delta$  ppm): 2.77 (s, 3H, (Ar)–C–H), 6.40 (s, 1H, (NH)–C–H), 6.67–6.86 (m, 4H, Ar–C–H), 7.20–7.43 (m, 3H, Ar–C–H), 8.06 (s, 2H, NH).  $^{13}\text{C}$  NMR ( $\text{DMSO}-d_6$ ,  $\delta$  ppm): 20.44, 45.13, 104.90, 115.24, 115.82, 121.13, 122.85, 126.80, 129.47, 129.75, 130.61, 132.81, 142.83, 150.23, 160.74, 161.35.

4-Phenyl-3,4-dihydro-1H-chromino[4,3-d]pyrimidine-2,5-dione (**5a**) IR (KBr,  $\text{cm}^{-1}$ ): 3,435 (N–H), 3,069 (aromatic C–H stretch), 1,658 (C=O), 1,566 (aromatic C=C bending).  $^1\text{H}$  NMR ( $\text{CDCl}_3$ ,  $\delta$  ppm): 6.06 (s, 1H, (NH)–C–H), 7.18–7.34 (m, 5H, Ar–C–H), 7.41–7.64 (m, 2H, Ar–C–H), 8.02–8.06 (m, 2H, Ar–C–H), 11.29 (s, 1H, NH), 11.56 (s, 1H, NH).  $^{13}\text{C}$  NMR ( $\text{DMSO}-d_6$ ,  $\delta$  ppm): 35.69, 104.22, 115.93, 117.03, 123.80, 123.84, 125.76, 126.50, 127.71, 128.04, 129.29, 132.00, 138.38, 152.04, 162.97, 164.42, 165.23.

4-(4-Methoxy)phenyl-3,4-dihydro-1H-chromino[4,3-d]pyrimidine-2,5-dione (**5b**) IR (KBr,  $\text{cm}^{-1}$ ): 3,069 (N–H), 2,835 (aromatic C–H stretch), 1,670 (C=O), 1,564 (aromatic C=C bending), 1,178 (C–O).  $^1\text{H}$  NMR ( $\text{CDCl}_3$ ,  $\delta$  ppm): 3.80 (s, 3H, (O)–C–H), 6.05 (s, 1H, (NH)–C–H), 6.87–7.41 (m, 4H, Ar–C–H), 7.63–8.05 (m, 4H, Ar–C–H), 11.31–11.52 (s, 2H, NH).  $^{13}\text{C}$  NMR ( $\text{DMSO}-d_6$ ,  $\delta$  ppm): 35.19, 54.92, 104.54, 113.57, 116.04, 117.30, 123.79, 123.95, 127.77, 130.66, 132.11, 152.06, 157.44, 164.45, 164.90.

4-(3,4-Dimethoxy)phenyl-3,4-dihydro-1H-chromino[4,3-d]pyrimidine-2,5-dione (**5c**) IR (KBr,  $\text{cm}^{-1}$ ): 3,461 (N–H), 2,837 (aromatic C–H stretch), 1,664 (C=O), 1,564 (aromatic C=C bending), 1,140 (C–O).  $^1\text{H}$  NMR ( $\text{CDCl}_3$ ,  $\delta$  ppm): 3.73 (s, 3H, (O)–C–H), 3.87 (s, 3H, (O)–C–H), 6.08 (s, 1H, (NH)–C–H), 6.71–7.80 (m, 3H, Ar–C–H), 7.63–8.06 (m, 4H, Ar–C–H), 11.31–11.53 (s, 2H, NH).  $^{13}\text{C}$  NMR ( $\text{DMSO}-d_6$ ,  $\delta$  ppm): 35.36, 55.40, 55.58, 104.47, 111.01, 111.35, 115.94, 116.98, 118.73, 123.73, 123.85, 130.63, 131.97, 147.23, 148.55, 152.02, 164.22, 165.13.

4-(4-Methoxy)phenyl-9-methyl-3,4-dihydro-1H-chromino[4,3-d]pyrimidine-2,5-dione (**5d**) IR (KBr,  $\text{cm}^{-1}$ ): 3,260 (N–H), 2,930 (aromatic C–H stretch), 1,624 (C=O), 1,575 (aromatic C=C bending), 1,149 (C–O).  $^1\text{H}$  NMR ( $\text{DMSO}-d_6$ ,  $\delta$  ppm): 2.45 (s, 3H, (Ar)–C–H), 3.79 (s, 3H, (O)–C–H), 6.02 (s, 1H, (NH)–C–H), 6.85–7.29 (m, 4H, Ar–C–H), 7.41 (s, 1H, Ar–C–H), 7.78–7.83 (m, 2H, Ar–C–H), 11.33–11.55 (s, 2H, NH).  $^{13}\text{C}$  NMR ( $\text{DMSO}-d_6$ ,  $\delta$  ppm): 20.45, 54.97, 104.48, 113.60, 115.87, 116.91, 123.43, 127.74, 130.57, 133.02, 133.28, 150.22, 157.48, 164.38, 165.11.

4-(3,4-Dimethoxy)phenyl-9-methyl-3,4-dihydro-1H-chromino[4,3-d]pyrimidine-2,5-dione (**5e**) IR (KBr,  $\text{cm}^{-1}$ ): 3,280 (N–H), 2,930 (aromatic C–H stretch), 1,664 (C=O), 1,564 (aromatic C=C bending), 956 (C–Br).  $^1\text{H}$  NMR ( $\text{DMSO}-d_6$ ,  $\delta$  ppm): 2.44 (s, 3H, (Ar)–C–H), 3.72 (s, 3H, (O)–C–H), 3.86 (s, 3H, (O)–C–H), 6.04 (s, 1H, (NH)–C–H), 6.68–6.78 (m, 2H, Ar–C–H), 7.30–7.41 (s, 2H, Ar–C–H), 7.77–7.83 (m, 2H, Ar–C–H), 11.32–11.56 (s, 2H, NH).  $^{13}\text{C}$  NMR ( $\text{DMSO}-d_6$ ,  $\delta$  ppm): 20.51, 55.39, 55.57, 104.43, 110.95, 111.36, 115.78, 116.49, 118.69, 123.34, 130.45, 132.97, 133.27, 147.24, 148.56, 150.16, 164.01, 165.32.

4-(4-Hydroxy-3-methoxy)phenyl-3,4-dihydro-1H-chromino[4,3-d]pyrimidine-2,5-dione (**5f**) IR (KBr,  $\text{cm}^{-1}$ ): 3,497 (O–H), 3,069 (N–H), 2,939 (aromatic C–H stretch), 1,668 (C=O), 1,564 (aromatic C=C bending), 1,151 (C–O).  $^1\text{H}$  NMR ( $\text{CDCl}_3$ ,  $\delta$  ppm): 3.74 (s, 1H, O–H), 5.60 (s, 3H, (O)–C–H), 6.06 (s, 1H, (NH)–C–H), 6.68–6.85 (m, 3H, Ar–C–H), 7.62–8.03 (m, 4H, Ar–C–H), 11.29–11.52 (s, 2H, NH).  $^{13}\text{C}$  NMR ( $\text{DMSO}-d_6$ ,  $\delta$  ppm): 35.59, 55.86, 104.74, 111.75, 115.29, 116.10, 117.35, 119.23, 123.79, 123.99, 129.65, 132.11, 144.98, 147.52, 152.10, 164.33, 164.84.

4-(2-Hydroxy)phenyl-3,4-dihydro-1H-chromino[4,3-d]pyrimidine-2,5-dione (**5g**) IR (KBr,  $\text{cm}^{-1}$ ): 3,393 (O–H), 3,065 (N–H), 1,672 (C=O), 1,560 (aromatic C=C bending), 1,105 (C–O).  $^1\text{H}$  NMR ( $\text{CDCl}_3$ ,  $\delta$  ppm): 3.74 (s, 1H, O–H), 5.37 (s, 1H, (NH)–C–H), 7.12–7.30 (m, 3H, Ar–C–H), 7.42–7.62 (m, 4H, Ar–C–H), 8.02–8.14 (s, 1H, Ar–C–H), 10.41 (s, 2H, NH).  $^{13}\text{C}$  NMR ( $\text{DMSO}-d_6$ ,  $\delta$  ppm): 48.65, 113.83, 116.02, 116.13, 116.29, 122.20, 122.50, 123.64, 124.23, 125.09, 128.09, 128.57, 131.82, 132.15, 151.98, 152.21, 160.40.

4-(3-Bromo)phenyl-3,4-dihydro-1H-chromino[4,3-d]pyrimidine-2,5-dione (**5h**) IR (KBr,  $\text{cm}^{-1}$ ): 3,280 (N–H), 2,930 (aromatic C–H stretch), 1,670 (C=O), 1,510 (aromatic C=C bending), 1,163 (C–O), 956 (C–Br).  $^1\text{H}$  NMR ( $\text{CDCl}_3$ ,  $\delta$  ppm): 6.06 (s, 1H, (NH)–C–H), 7.18–7.34 (m, 4H, Ar–C–H), 7.64–8.06 (m, 4H, Ar–C–H), 11.29–11.56 (s, 2H, NH).

$^{13}\text{C}$  NMR (DMSO- $d_6$ ,  $\delta$  ppm): 35.57, 103.84, 116.00, 116.86, 121.82, 123.83, 123.91, 125.66, 128.81, 129.24, 129.97, 132.15, 141.49, 152.06, 164.45, 165.10.

### Biological evaluation

Two methods were used for in vitro evaluation of anti-*M. tuberculosis* activity viz. (a) microplate Alamar blue assay (MABA) (Bartizal *et al.*, 1997; Scott *et al.*, 2007) and (b) luminescence-based low oxygen-recovery assay (LORA) (Scott *et al.*, 2007).

#### Microplate Alamar blue assay (MABA)

MABA is a sensitive, rapid, inexpensive, and non-radio-metric method that offers the potential for screening, with or without analytical instrumentation, a large number of anti-microbial compounds against slow-growing mycobacteria.

The Alamar blue oxidation–reduction dye is a general indicator of cellular growth and/or viability; the blue, non-fluorescent, oxidized form becomes pink and fluorescent upon reduction by the reducing power of living cells to convert resazurin to the fluorescent molecule, resorufin. Growth can therefore be measured with a spectrophotometer or determined by a visual color change thereby generating a quantitative measure of viability and cytotoxicity.

#### Materials and methods

**Bacterial strains and growth conditions** *Mycobacterium tuberculosis* H37Rv ATCC 27294 (H37Rv) was obtained from the American Type Culture Collection (Rockville, MD, USA). H37Rv inocula was first passaged in radiometric 7H12 broth (BACTEC 12B; Becton Dickinson Diagnostic Instrument Systems, Sparks, NV, USA) until the GI reached 800–999.

H37Rv was grown in 100 ml Middlebrook 7H9 broth (Difco, Detroit, MI, USA) supplemented with 0.2 % (v/v) glycerol (Sigma Chemical Co., Saint Louis, MO, USA), 10 % (v/v) oleic acid, albumin, dextrose, catalase (OADC; Difco), and 0.05 % (v/v) Tween 80 (Sigma, USA). The complete medium is referred to as 7H9GC-Tween. The culture was incubated in 500-ml nephelometer flasks on a rotary shaker (New Brunswick Scientific, Edison, NJ, USA) at 150 rpm and 37 °C until it reached an optical density of 0.4–0.5 at 550 nm. Bacteria were washed and suspended in 20 ml of phosphate-buffered saline and passed through 8-mm-pore-size filter to eliminate clumps.

**Chemicals and media** Rifampicin (RMP) and Clofazamine (CLF) were purchased from Sigma Chem. Co., USA. They were solubilized according to the manufacturer's recommendations and stock solutions were filter sterilized

(0.22 mm pore size) and stored at –80 °C. Alamar blue solution was purchased from Alamar Biosciences/Accumed, Westlake, OH, USA. Black, clear-bottomed, 96-well microplates (black view plates) were purchased from Packard Instrument Company, Meriden, CT, USA, in order to minimize background fluorescence. Fluorescence was measured in a Cytofluor II microplate fluorometer purchased from Perseptive Biosystems, Framingham, MA, USA.

**Alamar blue susceptibility test (MABA)** Antimicrobial susceptibility testing was performed in black, clear-bottomed, 96-well microplates in order to minimize background fluorescence. Outer perimeter wells were filled with sterile water to prevent dehydration in experimental wells. Initial drug dilutions were prepared in either dimethyl sulfoxide or distilled deionized water and subsequent two-fold dilutions were performed in 0.1 ml of 7H9GC (no Tween 80) in the microplates. BACTEC 12B-passaged inocula were initially diluted 1:2 in 7H9GC and 0.1 ml was added to the wells. Frozen inocula were initially diluted 1:20 in BACTEC 12B medium followed by a 1:50 dilution in 7H9GC. Wells containing drug only were used to detect auto-fluorescence of compounds. Additional control wells consisted of bacteria only (B) and medium only (M). Plates were incubated at 37 °C. Starting at day 4 of incubation, 20 ml of Alamar Blue solution and 12.5 ml of 20 % Tween 80 were added to one B well and one M well, and plates were re-incubated at 37 °C. Wells were observed at 12 and 24 h for a color change from blue to pink and for a reading of 50,000 fluorescence units (FU). Fluorescence was measured in a Cytofluor II microplate fluorimeter in bottom-reading mode with excitation at 530 nm and emission at 590 nm. If the B wells became pink by 24 h, reagent was added to the entire plate. If the well remained blue or 50,000 FU was measured, additional M and B wells were tested daily until a color change occurred, at which time reagents were added to all remaining wells. Plates were then incubated at 37 °C, and results were recorded at 24-h post-reagent addition. Visual MICs were defined as the lowest concentration of drug that prevented a color change. For fluorometric MICs, a background subtraction was performed on all wells with a mean of triplicate micro-wells. Percent inhibition defined as the lowest drug concentration effecting an inhibition of 90 % was considered as MIC.

#### Luminescence-based LORA

Screening for new antimicrobial agents is routinely conducted only against actively replicating bacteria. However, it is now widely accepted that a physiological state of NRP is responsible for antimicrobial tolerance in many bacterial infections. In tuberculosis, the key to shortening the 6-month regimen lies in targeting this NRP subpopulation.

Therefore, a high-throughput, luminescence-based LORA was developed to screen antimicrobial agents against NRP *M. tuberculosis*.

#### Materials and methods

**Construction of plasmid *luxAB*** The recombinant shuttle vector pFCA-*luxAB* was constructed by inserting the *luxAB* gene from pSMT1 into pFPCA1, which uses the acetamidase promoter to provide an enhanced signal. The *luxAB* genes were derived by PCR amplification with primers P1 (TAG GATCCTAAGAAAGATGAAATTTGGAAACTTCC) and P2 (TTCTTTAAATTACGAGTGGTATTTGACGATGTT GG). The amplified PCR product was cloned into the pGEM-T easy vector (Promega). After an *Escherichia coli* clone containing pGEMT-*luxAB* was obtained, the isolated plasmid was extracted and digested with BamHI and EcoRI. Following the ligation reaction with pFPCA1, the resulting plasmid, pFCA-*luxAB*, was used to transform *E. coli*. The plasmid was isolated, and the structure was confirmed by restriction enzyme digestion and sequencing analysis.

**Electroporation of plasmid pFCA-*luxAB* into *M. tuberculosis* H37Rv ATCC 27294** *Mycobacterium tuberculosis* H37Rv ATCC 27294 was obtained from the American Type Culture Collection (Manassas, VA, USA). After 5–7 days of culture in 200 ml Middlebrook 7H9 medium supplemented with oleic acid–albumin–dextrose–catalase, the cells were washed and transformed by mixing at least 1.0 g of purified plasmid and incubating at room temperature for 30 min, followed by electroporation. The transformants were cultured on Middlebrook 7H11 agar containing 20 g/ml kanamycin for 4 weeks. Selected colonies were transferred to 100 l of Middlebrook 7H9 broth and sonicated at 30 W for 20 s. (model S3000; Misonix Inc.) at ambient temperature prior to the measurement of the luminescence.

**Growth conditions** For the fermenter culture, recombinant H37Rv (pFCA*luxAB*) was grown to NRP phase 2 (NRP-2) in 300 ml of Dubos Tween albumin broth (Becton Dickinson) in a BioStat Q fermenter (B. Braun Biotech) to mimic the Wayne oxygen-limited culture with a headspace ratio (HSR) of 0.5 and agitated at a stir rate of 120 rpm with no detectable perturbation of the surface of the medium, as described previously. The fermenter culture was operated and maintained within a bio-safety level-3 laboratory. The dissolved oxygen concentration (DOC) was continuously monitored with an In-gold oxygen sensor probe. The optical densities of the cultures at 570 nm (A570 values), the numbers of relative light units (RLUs) and the CFU levels were determined at 3-day intervals. Bacterial samples were removed through a silicone septum with a syringe in order to preclude the introduction of

oxygen. The number of CFU was estimated by plating dilutions of aliquots on Dubos oleic-albumin agar plates in triplicate and incubating the cultures at 37 °C. The colonies were enumerated every week for 5 weeks. The cells were harvested at the 22nd day, a time when the A570 and DOC readings indicated achievement of the desired growth phase (NRP-2). 50 ml aliquots of bacterial culture samples were centrifuged (2,700×g, 30 min, 4 °C), washed once with pre chilled phosphate-buffered saline (PBS; pH 7.4), suspended in 1 ml of PBS, and stored at –80 °C.

**In vitro LORA and conventional aerobic culture assay** Prior to use, the cultures were thawed, diluted in Middlebrook 7H12 broth (Middlebrook 7H9 broth containing 1.0 mg/ml casitone, 5.6 g/ml palmitic acid, 5.0 mg/ml bovine serum albumin, and 4.0 g/ml filter-sterilized catalase), and sonicated for 15 s. For LORA, the microplate cultures were placed under anaerobic conditions (oxygen concentration, <0.16 %) using an Anoxomat model WS-8080 (MART Microbiology) and three cycles of evacuation and filling with a mixture of 10 % H<sub>2</sub>, 5 % CO<sub>2</sub>, and the balance N<sub>2</sub>. An anaerobic indicator strip was placed inside the chamber to visually confirm the removal of oxygen. The plates were incubated at 37 °C for 10 days and then transferred to an ambient gaseous condition (5 % CO<sub>2</sub>-enriched air) incubator for a 28 h “recovery.” The numbers of CFU (determined by subculture onto Middlebrook 7H11 agar) during the 10-day incubation did not increase and remained essentially unchanged. On day 11 (after the 28 h aerobic recovery), 100-l culture was transferred to white 96-well microtiter plates for determination of luminescence. For the conventional assay, the microplate cultures were placed in an incubator under ambient gaseous conditions (5 % CO<sub>2</sub> enriched air) for 7 days and 100-l culture was transferred to white 96-well microtiter plates for determination of luminescence. A 10 % solution of *n*-decanal aldehyde (Sigma) in ethanol was freshly diluted tenfold in PBS, and 100 l was added to each well with an auto-injector. Luminescence was measured in a Victor2 multi label reader (Perkin-Elmer Life Sciences) using a reading time of 1 s. The MIC defined as the lowest drug concentration effecting growth inhibition of 90 % relative to the growth for the drug-free controls.

#### Computational studies

RP analysis was carried out using the CSAR RP method and the decision tree was generated from the results of RP. *Cerius2* molecular modeling software was used to calculate the 2D descriptors for the molecules. The correlation matrices were built for the descriptors and those with zero variance as well as containing 95 % of zero values were eliminated. These remaining descriptors formed the independent variables (X), while the biological activity/toxicity

served as the dependent variable (Y) for the analysis. The CARTTM (classification and regression trees) method was applied to generate the decision tree classification model. The active and inactive classes (toxic and less toxic for the toxicity model) were given equal weight and the splits were scored using Twoing rule scoring function. The pruning factor was varied between 0 and 3. Maximum tree depth (layers <10) was also varied between 5 and 10, while the default values were set for maximum number of generic splits (30) and the number of knots per variable (20). The decision tree model was internally validated by cross-validation with the number of cross-validation groups set to 10.

**Acknowledgments** The computational, synthetic, and evaluation studies were possible due to the grants received from the All India Council for Technical Education (F. nos. 8022/RID/NPROJ/RPS-5/2003-04 and 8023/BOR/RID/RPS-181/2008-09), Department of Biotechnology (File no. BT/PR11810/BRB/10/690/2009), Council for Scientific Research (File no. 01/2399/10/EMRII) New Delhi and University of Mumbai (F. no. APD/237/157/2010).

## References

- Amaral L, Kristiansen JE, Viveiros M, Atouguia J (2001) Activity of phenothiazines against antibiotic-resistant *Mycobacterium tuberculosis*: a review supporting further studies that may elucidate the potential use of thioridazine as anti-tuberculosis therapy. *J Antimicrob Chemother* 47:505
- Barry VC, Belton JG, Conalty ML, Denneny JM, Edward DW, O'Sullivan JF, Twomey D, Winder F (1957) A new series of phenazines (rimino-compounds) with high antituberculosis activity. *Nature* 179:1013
- Bartizal K, Gill CJ, Abruzzo GK, Flattery AM, Kong L, Scott PM, Smith JG, Leighton CE, Bouffard A, Dropinski JF, Balkovec J (1997) In vitro preclinical evaluation studies with the echinocandin antifungal MK-0991 (L-743,872). *Antimicrob Agents Chemother* 41:2326
- Blower P, Fligner M, Verducci J, Bjoraker J (2002) On combining recursive partitioning and simulated annealing to detect groups of biologically active compounds. *J Chem Inf Comput Sci* 42:393
- Choi SY, Shin JH, Ryu CK, Nam KY, No KT, Park Choo HY (2006) The development of 3D-QSAR study and recursive partitioning of heterocyclic quinone derivatives with antifungal activity. *Bioorg Med Chem* 14:1608
- Cohen FL, Tartasky D (1997) Microbial resistance to drug therapy: a review. *Am J Infect Control* 25:51
- Desai B, Sureja D, Naliapara Y, Shah A, Saxena AK (2001) Synthesis and QSAR studies of 4-substituted phenyl-2,6-dimethyl-3, 5-bis-N-(substituted phenyl)carbamoyl-1,4-dihydropyridines as potential antitubercular agents. *Bioorg Med Chem* 9:1993
- Garcia-Garcia A, Galvez J, de Julian-Ortiz JV, Garcia-Domenech R, Munoz C, Guna R, Borrás R (2005) Search of chemical scaffolds for novel antituberculosis agents. *J Biomol Screen* 10:206
- Jarvis B, Lamb HM (1998) Rifapentine. *Drugs* 56:607
- Jindani A, Aber VR, Edwards EA, Mitchison DA (1980) The early bactericidal activity of drugs in patients with pulmonary tuberculosis. *Am Rev Respir Dis* 121:939
- Kawakami K, Namba K, Tanaka M, Matsuhashi N, Sato K, Takemura M (2000) Antimycobacterial activities of novel levofloxacin analogues. *Antimicrob Agents Chemother* 44:2126
- Kidwai M, Saxena S, Mohan R (2006) Environmentally benign synthesis of benzopyranopyrimidines. *Russ J Org Chem* 42:52. doi:10.1134/s107042800601009x
- Krajewski WW, Jones TA, Mowbray SL (2005) Structure of *Mycobacterium tuberculosis* glutamine synthetase in complex with a transition-state mimic provides functional insights. *Proc Natl Acad Sci USA* 102:10499–10504
- Manvar A, Malde A, Verma J, Virsodia V, Mishra A, Upadhyay K, Acharya H, Coutinho E, Shah A (2008) Synthesis, antitubercular activity and 3D-QSAR study of coumarin-4-acetic acid benzylidene hydrazides. *Eur J Med Chem* 43:2395
- Manvar AT, Pissurlenkar RR, Virsodia VR, Upadhyay KD, Manvar DR, Mishra AK, Acharya HD, Parecha AR, Dholakia CD, Shah AK, Coutinho EC (2010) Synthesis, in vitro antitubercular activity and 3D-QSAR study of 1,4-dihydropyridines. *Mol Divers* 14:285. doi:10.1007/s11030-009-9162-8
- Marinis E, Legakis NJ (1985) In-vitro activity of ciprofloxacin against clinical isolates of mycobacteria resistant to antimycobacterial drugs. *J Antimicrob Chemother* 16:527
- McKee TC, Covington CD, Fuller RW, Bokesch HR, Young S, Cardellina II, Kadushin MR, Soejarto DD, Stevens PF, Cragg GM, Boyd MR (1998) Pyranocoumarins from tropical species of the genus *Calophyllum*: a chemotaxonomic study of extracts in the National Cancer Institute collection. *J Nat Prod* 61:1252. doi:10.1021/np980140anp980140a
- Miyakawa Y, Ratnakar P, Rao AG, Costello ML, Mathieu-Costello O, Lehrer RI, Catanzaro A (1996) In vitro activity of the antimicrobial peptides human and rabbit defensins and porcine leukocyte protegrin against *Mycobacterium tuberculosis*. *Infect Immun* 64:926
- Rusinko A III, Young SS, Drewry DH, Gerritz SW (2002) Optimization of focused chemical libraries using recursive partitioning. *Comb Chem High Throughput Screen* 5:125
- Ryabukhin SV, Plaskon AS, Boron SY, Volochnyuk DM, Tolmachev AA (2011) Aminoheterocycles as synthons for combinatorial Biginelli reactions. *Mol Divers*. doi:10.1007/s11030-010-9253-6
- Scott GM, Weinberg A, Rawlinson WD, Chou S (2007) Multidrug resistance conferred by novel DNA polymerase mutations in human cytomegalovirus isolates. *Antimicrob Agents Chemother* 51:89. doi:AAC.00633-06
- Shiradkar M, Suresh Kumar GV, Dasari V, Tatikonda S, Akula KC, Shah R (2007) Clubbed triazoles: a novel approach to antitubercular drugs. *Eur J Med Chem* 42:807
- Spino C, Dodier M, Sotheeswaran S (1998) Anti-HIV coumarins from *Calophyllum* seed oil. *Bioorg Med Chem Lett* 8:3475
- Stover CK, Warrenner P, VanDevanter DR, Sherman DR, Arain TM, Langhorne MH, Anderson SW, Towell JA, Yuan Y, McMurray DN, Kreiswirth BN, Barry CE, Baker WR (2000) A small-molecule nitroimidazopyran drug candidate for the treatment of tuberculosis. *Nature* 405:962. doi:10.1038/35016103
- Strobl C, Malley J, Tutz G (2009) An introduction to recursive partitioning: rationale, application, and characteristics of classification and regression trees, bagging, and random forests. *Psychol Methods* 14:323
- Virsoia V, Shaikh MS, Manvar A, Desai B, Parecha A, Loriya R, Dholariya K, Patel G, Vora V, Upadhyay K (2010) Screening for in vitro antimycobacterial activity and three dimensional quantitative structure–activity relationship (3D QSAR) Study of 4 (arylamino) coumarin derivatives. *Chem Bio Drug Design* 76:412
- Xu Z-Q, Barrow WW, Suling WJ, Westbrook L, Barrow E, Lin Y-M, Flavin MT (2004) Anti-HIV natural product (+)-calanolide A is active against both drug-susceptible and drug-resistant strains of *Mycobacterium tuberculosis*. *Bioorg Med Chem* 12:1199
- Young SS, Hawkins DM (2004) Using recursive partitioning analysis to evaluate compound selection methods. *Methods Mol Biol* 275:317